



## A SOFTWARE TO DIGITAL IMAGE PROCESSING TO BE USED IN THE VOXEL PHANTOM DEVELOPMENT

J. W. VIEIRA<sup>1, 2, 3</sup> AND F. R. A. LIMA<sup>3</sup>

<sup>1</sup> Instituto Federal de Educação, Ciência e Tecnologia de Pernambuco, Av. Prof. Luiz Freire, 500, Curado, Recife-PE, Brasil

<sup>2</sup> Escola Politécnica de Pernambuco – UPE, Rua Benfica, 455, CEP 50750-470 Madalena, Recife-PE, Brasil

<sup>3</sup> Centro Regional de Ciências Nucleares – CRCN, Av. Prof. Luiz Freire, 200

Cidade Universitária, Recife-PE, Brasil, CEP 50740-540

✉ Fax: Email: jwvieira@br.inter.net

*Received, September 1<sup>st</sup> 2008; Accepted October 1<sup>st</sup>, 2009; Published November 15<sup>th</sup>, 2009*

**Abstract** – Anthropomorphic models used in computational dosimetry, also denominated phantoms, are based on digital images recorded from scanning of real people by Computed Tomography (CT) or Magnetic Resonance Imaging (MRI). The voxel phantom construction requests computational processing for transformations of image formats, to compact two-dimensional (2-D) images forming of three-dimensional (3-D) matrices, image sampling and quantization, image enhancement, restoration and segmentation, among others. Hardly the researcher of computational dosimetry will find all these available abilities in single software, and almost always this difficulty presents as a result the decrease of the rhythm of his researches or the use, sometimes inadequate, of alternative tools. The need to integrate the several tasks mentioned above to obtain an image that can be used in an exposure computational model motivated the development of the Digital Image Processing (DIP) software, mainly to solve particular problems in Dissertations and Thesis developed by members of the Grupo de Pesquisa em Dosimetria Numérica (GDN/CNPq). Because of this particular objective, the software uses the Portuguese idiom in their implementations and interfaces. This paper presents the second version of the DIP, whose main changes are the more formal organization on menus and menu items, and menu for digital image segmentation. Currently, the DIP contains the menus Fundamentos, Visualizações, Domínio Espacial, Domínio de Frequências, Segmentações and Estudos. Each menu contains items and sub-items with functionalities that, usually, request an image as input and produce an image or an attribute in the output. The DIP reads edits and writes binary files containing the 3-D matrix corresponding to a stack of axial images from a given geometry that can be a human body or other volume of interest. It also can read any type of computational image and to make conversions. When the task involves only an output image, this is saved as a JPEG file in the Windows default; when it involves an image stack, the output binary file is denominated SGI (Simulações Gráficas Interativas (Interactive Graphic Simulations), an acronym already used in other publications of the GDN/CNPq.

**Key words:** Digital Image Processing, voxel phantom, computational dosimetry

### INTRODUCTION

Numeric dosimetry uses exposure models to estimate the absorbed dose in the exposed body to the radiation. Some exposure computational models were developed by the GDN (Grupo de Pesquisa em Dosimetria Numérica) for applications in radiation protection (1, 2, 3, 4), accidents (5), diagnostic radiology (6, 7) and Nuclear Medicine (8). Anthropomorphic simulators used in these and other several papers were developed starting from CT images submitted to several transformations until constitute 3-D matrices representing virtual human bodies with the masses of the organs and tissues in risk recommended by ICRP (9). Many of these transformations were edited in FANTO-

MAS software (10, 11) and also in the first version of DIP (12).

The need to integrate the several processing tasks of the original digital image to obtain an image that can be used in the computational model motivated the development of the DIP software. This software was developed in C++, using the project template Windows Form Application (.NET) of Visual Microsoft Studio .NET 2003 (13), to read, to edit and to write binary files containing the 3-D matrix corresponding to a stack of axial images of a given geometry that can be a human body or other volume of interest. The software also can read any type of computer image (BMP, JPEG, TIF etc.) and to make conversions for the default types used in tasks implemented in it. When the task just involves an output image, this is saved

as a JPEG file; when it involves a stack of images, the resulting binary file is denominated SGI. To the stacks of images established they are called voxel phantom or SGI-phantom. In this paper is presented, based on menus and menu items, the second version of the DIP software that is available for computational dosimetry researchers (jwvieira@br.inter.net) in an installation package (DIPSetup) containing three files: DIPSetup.msi, Setup.ini and Setup.exe. A double click on the file Setup.exe can install the software in a similar way to be used in Windows programs. For computers where it is not still installed the .NET Framework, in the beginning of the installation it will appear the electronic address presented in the reference (14). The user should find in this address the file dotnetfx.exe, which contains all the necessary tools to execute applications developed with .NET Framework. The user should to download and to install the dotnetfx.exe in your computer for, then, to continue in the DIP installation.

The yield of the installation is two files: dip.exe and a file \*.pdf with the paper that presents the first version of DIP (12).

## MATERIALS AND METHODS

Figure 1 shows the main window of DIP, displaying the menu Fundamentos. The menu item selected converts an 8-bit binary file only containing raw data of the phantom (these files usually have extension \*.raw or \*.dat) in a stack DIP default, that is, a binary file with extension \*.sgi. These stacks contain an information header + the file \*.raw. The header contains the phantom dimensions in the following order: columns, lines, slices. Several types of conversions are available in the other sub-items shown in Figure 1. As an example, the file head256.raw, available in (15), can be converted into head256.sgi using the DIP path selected in Figure 1. This file contains 225 axial slices of a man's head, each one with area of 256 x 256 pixels. The data are stored with 1 byte/pixel and the resolution of voxel is of 1 mm. head256.sgi, used in several occasions along this text.

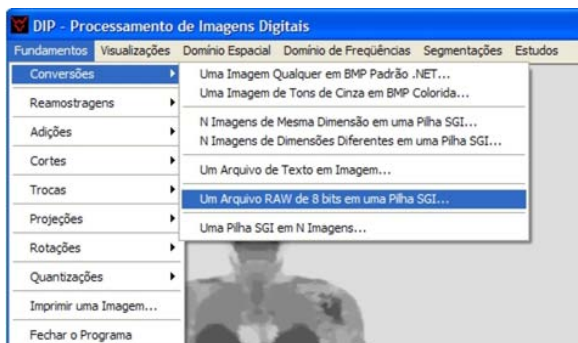


Figure 1. Main window of the DIP software

## FUNDAMENTOS MENU

Sampling and quantization (16) are the main fundamentals of digital image processing organized in this menu. Digitizing the coordinate values of the continuous image is called sampling. Resampling a digital image is to increase or to reduce its dimensions. Digitizing the amplitude values,  $f(x, y)$ , is called quantization. In section 2.2 are presented examples of resampling and quantization of digital images. Figure 2 shows the available sub-items for resampling in DIP. The selected example allows the access to the dialog box shown in Figure 3a where the user can type the column number (width in pixels) of the new image and to click in the button Aplicar... to obtain a SGI-phantom of images resampled without deformations. For this, the  $N^{\circ}$  Novo de Colunas /  $N^{\circ}$  Velho de Colunas factor is used for the other dimensions. At the end of the execution, the dialog box of Figure 3b is shown. This modality of input data is also common in the DIP software for two or three values. There is one class of the type Windows Forms Application (.NET) called SizeColunaLinhaFatia to control these inputs. The modality of output data exemplified is also very used in DIP. To open and to save files are used, in most of the interactions with the user, the native classes OpenFileDialog and SaveFileDialog (13).

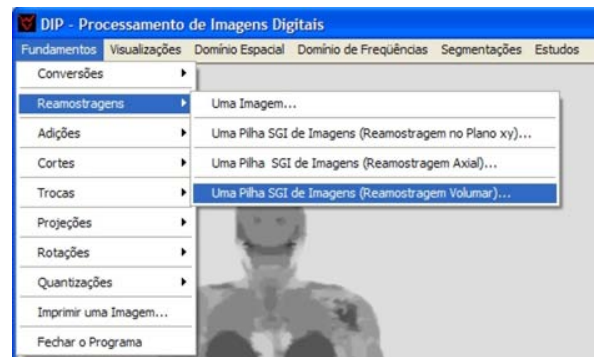


Figure 2. Digital image resampling in the DIP.



Figure 3. (a) Dialog box for resampling 3-D without deformations of a SGI-phantom based in column number. (b) Program calculates the other dimensions and exhibits them, adjusting the input SGI-phantom for the new volume.

## VISUALIZAÇÕES MENU

Figure 4a shows the available items in the Visualizações menu. If the user clicks in the option selected in the Figure 4a, he will see in the window of DIP a SGI-phantom. The slices of the stack are exhibited continually. If the user wants to stop the scrolling in the window it is enough he clicks with the left button of the mouse on the current image. New click with this button and the stack will continue the scrolling. Figure 4b shows, as an example, the slice 90 of the file head256.sgi. For to roll the stack, slice-by-slice, the pair of keys  $> / <$ , or the pair of arrow keys  $\uparrow / \downarrow$  can be used. If the user clicks now with the right button of the mouse on the image exhibited, he will access the context menu also shown in Figure 4b.



**Figure 4.** (a) Visualizações Menu. (b) Stack exhibited through the menu item selected in (a).

To exemplify the image resampling and quantization, the slice 90 shown in Figure 4b was saved with the name head256\_90.jpg. Figure 5 shows the original image with 256 x 256 pixels, and two resampling of the same: with 200 x 200 and 100 x 100 pixels. These new images were obtained through the menu item Fundamentos → Reamostragem → Uma Imagem... shown in Figure 2. To exhibit them, the menu item Visualizações → Uma ou Mais Imagens... shown in Figure 4a was used.

Figure 6 shows an original image, two quantization images for 16 and 4 gray-levels, and its respective histograms. The histograms were built accessing the DIP path Histograma → Uma Imagem → Com Fundo... shown in Figure 7.

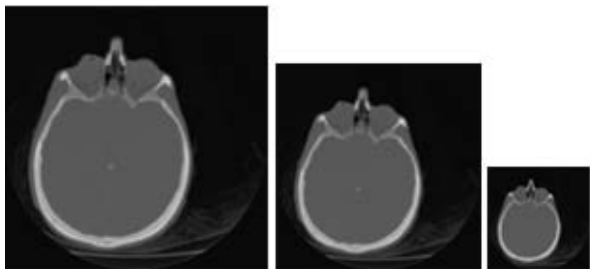


**Figure 5.** Image with 256 x 256 pixels, and resampling for 200 x 200 and 100 x 100.

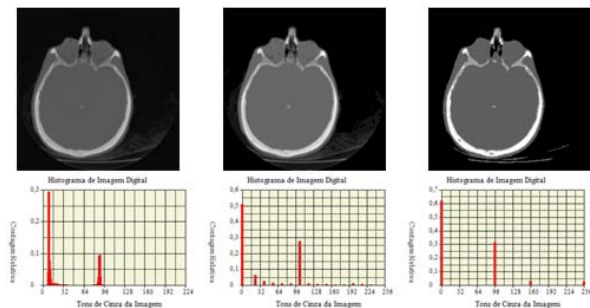


**Figure 6.** Original image, two quantization images for 16 and 4 gray-levels, and their respective histograms.



**Figure 7.** Menu items of the DIP to display an image and its histogram.

CT images of the human body contain a background that, for the development of anthropomorphic models, should be filled out by an only gray-level. The artifacts that appear in the background of Figure 6a can be eliminated by analyzing the histogram of the image and establishing a range of gray-levels for the background as a pre-processing. In the first line of Figure 8 are shown the Figure 6a and the result of the application on it of the replacement of the gray-levels smaller or equal to 48 by 0. This was made by accessing the DIP path Fundamentos → Trocas → Intervalo de Tons de Cinza por um Único Tom em uma Imagem... The same pre-processing was made for the stack head256.sgi, and the result was saved in the file head256\_Fundo(0,48).sgi. The second line of Figure 8 shows the histograms of the images of the first line. As one can see, now, almost all the pixels in the area of the background are zero.

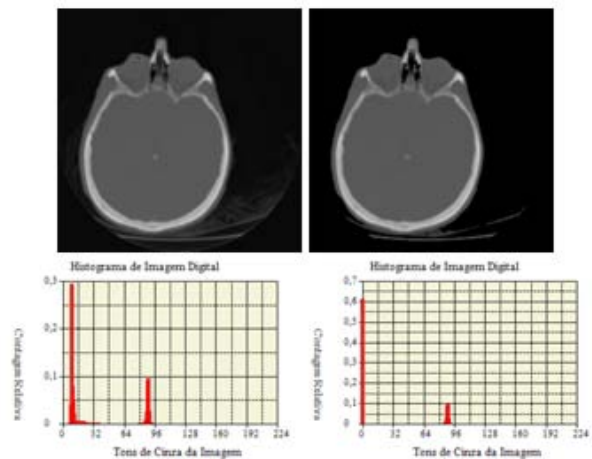


**Figure 8.** Original image, resulting image of the substitution of [0, 48] by 0, and its respective histograms.

In the sequence, are presented and used the techniques of digital image enhancement and restoration to eliminate the remaining artifacts.

### DOMÍNIO ESPACIAL MENU

This menu is the core of the DIP software version here presented. Figure 9 shows one of its ramifications. Almost all the algorithms about image enhancement and restoration in the space domain described in Gonzalez and Woods' book (16) were implemented in DIP and organized in this menu. In the sequence, some illustrative examples are presented.

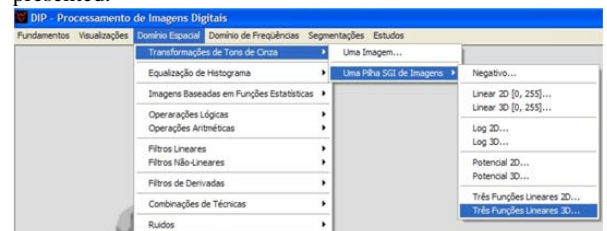


**Figure 9.** One of the ramifications of the Domínio Espacial menu.

### Transformations based in gray-levels

These transformations have as input a digital image with gray-levels  $r$ , and produce an output image with gray-levels  $s$ , where  $s = T(r)$ .

The example selected in Figure 9 is based on the transformation function shown in Figure 10a, which is a composition of three linear functions, and it is used for contrast stretching of images with narrow dynamic range. The locations of the points  $(r_1, s_1)$  and  $(r_2, s_2)$  control the shape of the transformation function. Figure 10b shows the gray-levels histogram of the average image of the stack head256\_Fundo(0,48).sgi (each gray-level is the average of gray-levels in the same position  $(x, y)$  of the 225 images of this SGI-phantom. The background was removed of the histogram). In agreement with this histogram, the dynamic range of the SGI-phantom is  $[48, 128]$  and, besides the background, there are two dominant areas in the 3-D matrix, corresponding to soft tissue and to bone. If the objective of the transformation were to segment the images, the expansion of the dynamic range can be an useful operation because it increases the contrast between the areas that one wants to identify. Figure 11a and 11b show the slice 90 of the files head256\_Fundo(0,48).sgi and head256\_48\_112.sgi. This last file was obtained using  $(r_1, s_1) = (48, 0)$  and  $(r_2, s_2) = (112, 255)$  in the dialog box opened when the user chooses the option selected in Figure 9. Note that, now, the bone area in Figure 11b is practically white what facilitates the segmentation of the head's bones in the complete stack.

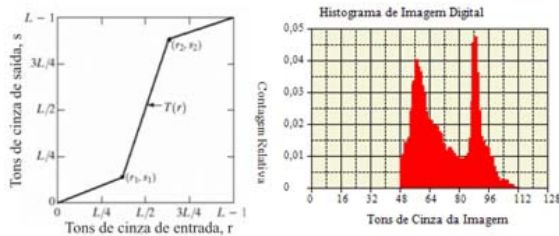


**Figure 10.** (a) Contrast-stretching transformation function. (b) Histogram (without background) of the average image of the stack head256\_Fundo(0,48).sgi.

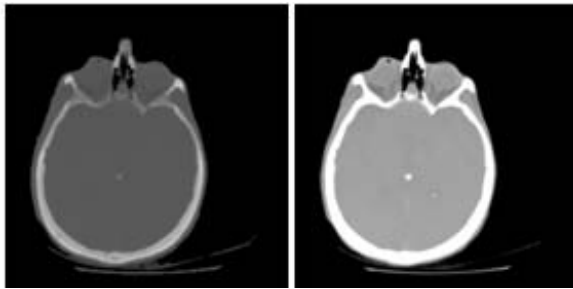


**Figure 11.** (a) Original image. (b) Contrast-stretching transformation resulting on the image (a) for  $(r_1, s_1) = (48, 0)$  and  $(r_2, s_2) = (112, 255)$ .

*Transformations based on Linear Operators*

Some operations of enhancement or restoration work with the values of image pixels around and the corresponding values of a subimage with the same dimensions as the areas around. The subimage is called a filter, mask, kernel, template or window. The values in a mask are referred as coefficients, rather than pixels.

The mechanics of spatial filtering consist on moving the mask from point to point in an image. At each point  $(x, y)$ , the local response is calculated using a predefined relationship.

The general implementation for filtering an  $M \times N$  image with a weighted averaging filter of size  $m \times n$  ( $m$  and  $n$  odd) is given by the expression:

$$g(x, y) = \frac{\sum_{s=-m/2}^{m/2} \sum_{t=-n/2}^{n/2} w(s, t) f(x + s, y + t)}{\sum_{s=-m/2}^{m/2} \sum_{t=-n/2}^{n/2} w(s, t)} \quad (1)$$

where  $x = 0, 1, \dots, M - 1, y = 0, 1, \dots, N - 1$ ,  $w$ 's are mask coefficients,  $f$  is the input image, and  $g$  is the output image.

If the user clicks in the DIP path Domínio Espacial → Filtros Lineares, he can use implementations of arithmetic, geometric, harmonic and contraharmonic mean filters, for an image or a SGI-phantom. In all these implementations it is necessary to enter with the filter size (odd integers smaller than the image size), and some other specific parameter for the mean type, to open and to transform the image or the stack, saving the result.

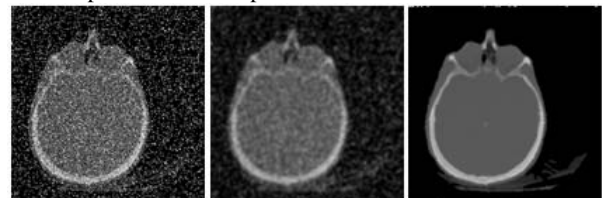
An important application of spatial averaging is to blur an image for the purpose getting a gross representation of the objects of interest contained in the image so that the intensity of smaller objects blends with the background and larger objects becomes "gray regions" of easy subsequent detection.

Figure 12a is the same image exhibited in Figure 11a where an impulse noise was added (also called salt-and-pepper. Some noise types can be added to an image through the DIP path Domínio Espacia → Ruídos → Adição de Ruídos) with probabilities of 20%. Figure 12b shows the result of the application of an arithmetic mean filter of size  $3 \times 3$  in Figure 12a. It sees that the processed image has less noise visible, but the price pays is that the image was blurrier.

*Transformations based on Nonlinear Operators*

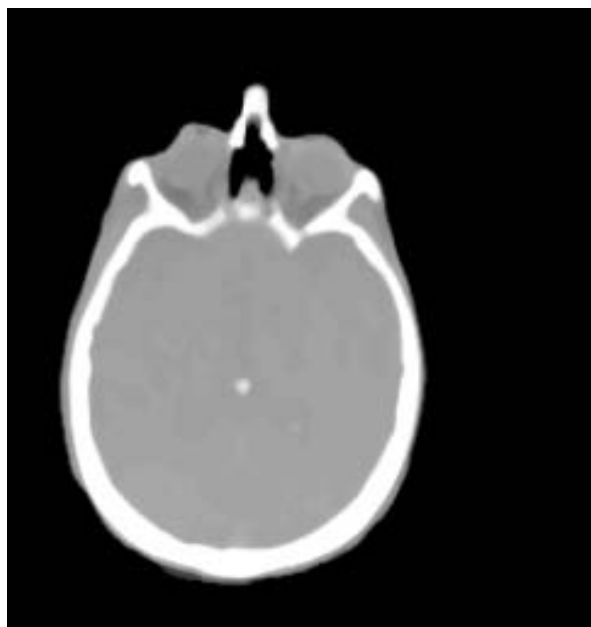
Nonlinear operators are transformations as accomplished them by the order-statistics filters, which are spatial filters whose response is based on ordering the pixels contained in the image area encompassed by the filter. The value of the central pixel is replaced by the value determined in the ranking process. The best-known order-statistics filter is the median filter, which, as its name implies, replaces the value of a pixel by the median of the gray levels around of that pixel (the original value of the pixel is included in the computation of the median). Median filters are quite popular because, for certain types of random noise, they provide excellent noise-reduction capabilities, with considerably less blurring than linear smoothing filters of similar size.

Figure 12c shows the result of the application of a  $3 \times 3$  median filter on the image of Figure 12a. In all the aspects, the superiority of median filter over the arithmetic mean filter in this case is quite evident. To use this and other nonlinear filters implemented in DIP, the user should access the DIP path Domínio Espacial → Filtros Não-Lineares.



**Figure 12.** (a) Image of Figure 11a additionally corrupted by salt-and-pepper noise. (b) Result of arithmetic mean filtering in image (a). (c) Result of median filtering in image (a).

To the image of Figure 11b it can be applied more two enhancements to eliminate the remaining artifacts: The median filtering repeated times, and new change of the gray levels smaller or equal to 48 for 0. Figure 13 shows the final result.



**Figure 13.** Image of Figure 11b after the median filtering and new adjust of the background.

As it is seen in the menu exhibited in Figure 9, there are several other techniques of image enhancement and/or restoration implemented in DIP software. For more details, the user should consult the paper of DIP previous version (12) or to get in touch with the authors.

The Domínio de Frequências menu is not commented in this paper.

In sequence, is presented an example of segmentation of the SGI-phantom from where was obtained the Figure 13.

#### SEGMENTAÇÕES MENU

Segmentation of SGI-Phantoms is an image analysis operation that aims at partitioning the voxels into 3-D regions that represent meaningful physical entities. In the example used in this paper, the regions of interest for dosimetric simulations could be skin, bone and brain. Such a classification into regions is performed by requiring voxels that belong to a certain region share some predefined properties with respect to a specific feature vector, which may include voxel characteristics like intensity, texture, spatial position, and proximity. It is obvious that segmentation is a crucial step in the sequence of operations preceding 3-D visualization and morphometric analysis, where its results are used to select the objects of interest among the several objects usually presented in a volume. Segmentation of SGI-Phantoms is also very important in the digital image processing, where it can be used as a preprocessing step in image sequence compression and in motion-compensated spatiotemporal filtering to simulate movements (17).

Some segmentation techniques were already included in the DIP software, into the ones which the merging region. This approach consists on constructing homogeneous regions through the merging of voxels having similar properties. According to the merging algorithm, the SGI-

Phantom is traversed in a columns-rows-slices model, namely by scanning the rows, column by column, of the  $k$ th slice before proceeding to the  $k + 1$  slice. The algorithm starts creating the first region, which contains the first voxel of the volume. Then, for each voxel traversed, merging with the regions around is attempted. Merging is decided if the current voxel intensity is close to the mean intensity of the region under consideration. After this, the mean intensity of the region is updated. When merging criteria are satisfied by more than one region, the region with the closest mean intensity is chosen. If no merging with the neighboring regions is possible, the algorithm tries to merge the current voxel with nonneighboring regions. Further failure to merge the voxel results in creation of a new region provided that the maximum number of regions has not been reached. The merging algorithm stops when all volume voxels have been visited.

The implementation of this algorithm in DIP was used to segment the SGI-Phantom resulting of the processes applied on SGI-Phantom contained in the head256.sgi file and described in the previous sections. Figure 14a shows the slice 90 of the segmented set (the colors were applied using the DIP path Fundamentos → Conversões → Uma Imagem de Tons de Cinza em BMP Colorida...). Finally, the SGI-Phantom was centralized (using the DIP path Fundamentos → Trocas → Centralização de Pilha SGI de Imagens Segmentadas...) and saved in file named head256\_segmentada\_centralizada.sgi. Figure 14b shows the slice 90 centralized.

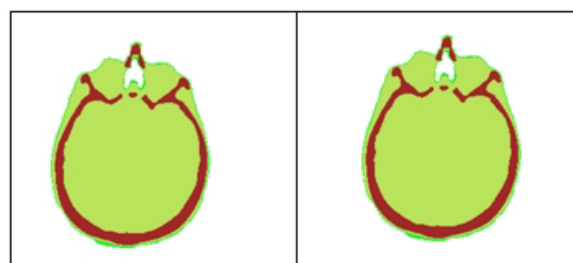


**Figure 14.** (a) Color image of Figure 13. (b) Figure (a) centralized.

#### ESTUDOS MENU

This menu contains items that allow access to SGI Phantom special manipulations for which are used in dissertation and these works (7, 8), and also in publications on skeletal dosimetry (18, 19). Other menu items will be added to this menu for development of students and researcher future works, who are members of GDN. One also plans to add a help menu to the DIP user in a next version.

## CONCLUSIONS AND PERSPECTIVES

In this paper the second version of the DIP software was presented by using some examples of its functionality, mainly the processing techniques related with digital image enhancement and restoration in the spatial domain, and a technique of SGI Phantom segmentation. The software was developed in Microsoft Visual Studio C++ .NET 2003 and it was already used in some studies of GDN and

also by other researchers from the Departamento de Energia Nuclear / Universidade Federal de Pernambuco. Whenever necessary, the DIP software is being updated to adjust new functionalities inherent to the new challenges.

One of the planned incorporations will allow the user to visualize surfaces of SGI Phantoms as shown in Figure 15. The images of this figure were obtained using the FantomasNURBS software (20) in development that integrates the user graphics interfaces of the Microsoft Visual Studio C++ .NET with the graphic library OpenGL (21) for construction of new voxel phantoms.

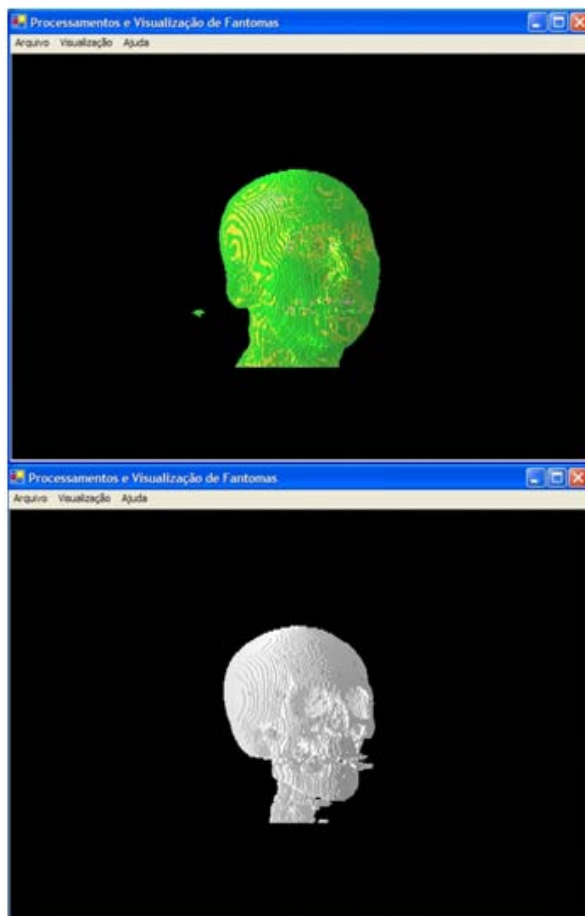


**Figure 15.** (a) View of the surface of the SGI Phantom head256\_segmentada\_centralizada.sgi. (b) Skull contained in the image stack (a).

## REFERENCES

- Kramer, R., Vieira, J. W., Khoury, H. J., Lima, F. R. A. and Fuelle, D., All about MAX: A Male Adult voXel Phantom for Monte Carlo Calculations in the Area of Radiation Protection Dosimetry, *Phys. Med. Biol.*, **48**, 1239-1262, (2003).
- Kramer, R., Vieira, J. W., Khoury, H. J., Lima, F. R. A., Loureiro, E. C. M, Lima, V. J. M. and Hoff, G., All about FAX: a Female Adult voXel Phantom for Monte Carlo Calculation in Radiation Protection Dosimetry, *Phys. Med. Biol.*, **49**, 5203-5216, (2004).
- Vieira, J. W., Construção de um Modelo Computacional de Exposição para Cálculos Dosimétricos Utilizando o Código Monte Carlo EGS4 e Fantomas de Voxels, Tese de Doutorado, DEN-UFPE, Recife-PE, Brasil, (2004).
- Kramer, R., Khoury, H. J., Vieira, J. W. and Lima V. J. M., MAX06 and FAX06: Update of Two Human Phantoms for Radiation Protection Dosimetry, *Phys. Med. Biol.*, **51**, 6265-6289, (2006).
- Santos, A. M., Desenvolvimento de um Modelo Computacional para Cálculos de Dose Absorvida em Órgãos e Tecidos do Corpo Humano em Situações de Exposições Acidentais, Tese de Doutorado, DEN-UFPE, Recife-PE, Brasil, (2006).
- Leal Neto, V., Desenvolvimento de uma Interface Gráfica de Usuário para Modelos Computacionais de Exposição Externa, Dissertação de Mestrado, DEN-UFPE, Recife-PE, Brasil, (2007).
- Costa, R. K. F., Radiografias Digitais Sintéticas Utilizando Modelos Computacionais de Exposição do Tipo FANTOMAS DE VOXELS/EGS4, Dissertação de Mestrado, DEN-UFPE, Recife-PE, Brasil, (2008).
- Lopes Filho, F. J., Avaliações Dosimétricas em Pacientes Submetidos à Radioiodoterapia com Base em Fantomas de Voxels e em Imagens de Medicina Nuclear, Tese de Doutorado, DEN-UFPE, Recife-PE, Brasil, (2007).
- International Commission on Radiological Protection, ICRP 89, Basic Anatomical and Physiological Data for Use in Radiological Protection: Reference Values, Pergamon Press, Oxford, (2003).
- Vieira, J. W., Stosic, B., Lima, F. R. A., Kramer, R., Santos, A. M. e Lima, V. J. M., Um Software para Editar Fantomas de Voxels e Calcular Coeficientes de Conversão para a Proteção Radiológica, Primeiro Congresso Brasileiro de Proteção Radiológica, Rio de Janeiro, 02 a 05 de novembro de 2005.
- Vieira, J. W., Santos, A. M. e Lima, F. R. A., Tratamento de Imagens Tomográficas para Uso em Dosimetria Numérica, Primeiro Congresso Americano do IRPA, Acapulco, México, 03 a 08 de setembro de 2006.
- Vieira J. W., Lima F. R. A., Santos A. M., Leal Neto V. e Lima V. J. M., DIP - Um Software para Processamento de Imagens Digitais, II Congresso de Pesquisa e Inovação da Rede Norte Nordeste de Educação Tecnológica – II CONNEPI, João Pessoa-PB, Brasil, 27 a 29 de novembro de 2007.
- Templeman, J. and Olsen, A., Microsoft Visual C++ .NET, Step by Step. Version 2003, Microsoft Press, USA, (2002).
- Microsoft .NET Framework Version 1.1 Redistributable Package, Download. Disponível em: <http://www.microsoft.com/downloads/details.aspx?familyid=262-D25E3-F589-4842-8157-034D1E7CF3A3&displaylang=en>, Acesso em 21 agosto de 2007.
- Engel, K., Pre-Integrated Volume Rendering, <http://wwwvis.informatik.uni-stuttgart.de/~engel/pre-integrated/data.html>, Última atualização em 20/04/2001. Acesso em março de 2008.
- Gonzalez, R. C. and Woods, R. E., Digital Image Processing, 2nd ed., Prentice Hall, Upper Saddle River, New Jersey, USA, (2002).
- Nikolaïdis, N and Pitas, I, 3-D Image Processing Algorithms, Wiley-Interscience, (2001).
- Kramer, R., Khoury, H. J., Vieira, J. W. and Kawrakow, I., Skeletal Dosimetry in the MAX06 and the FAX06 Phantoms for External Exposure to Photons Based on

- Vertebral 3-D-microCT Images, *Phys. Med. Biol.*, **51**, 6265-6289, (2006).
19. Kramer, R., Khoury, H. J., Vieira, J. W. and Kawrakow, I., Skeletal Dosimetry for External Exposure to Photons Based on  $\mu$ CT Images of Spongiosa from Different Bone Sites, *Phys. Med. Biol.*, **52**, 6697-6716, (2007).
20. Vieira, J. W., Desenvolvimento de Fantasmas de Voxels 4D a Partir de Curvas e Superfícies NURBS para Avaliações Dosimétricas, Projeto de Pesquisa de Pós-doutorado, em andamento no CRCN-CNEN, Recife-PE, Brasil, (2007).
21. Shreiner, D., Woo, M., Neider, J. and Davis, T., OpenGL Programming Guide The Official Guide to Learning OpenGL, Version 1.4, OpenGL Architecture Review Board, 4th ed., Addison-Wesley, USA, (2004).
22. Araujo F., Rebelo A. M. O., Pereira A. C., Moura M. B., Lucena E. A., Dantas A. L. A., Dantas B. M. and Corbo R., Optimization of  $^{131}\text{I}$  doses for the treatment of hyperthyroidism. *Cell. Mol. Biol.* 2009, **55**: 1-6.
23. Santos A. M. and Vieira J. W., 'Voxelization' of alderson-rando phantom for use in numerical dose measuring. *Cell. Mol. Biol.* 2009, **55**: 7-12.
24. Cardoso J. C. S., Berti e. A. R. and Xavier M., Whole-body measurements at IPEN, Brazil. *Cell. Mol. Biol.* 2009, **55**: 13-14.
25. Holanda C. M. C. X., Silva-Júnior m. F., Alves R. C., Barbosa V. S. A., Silva R. P., Rocha L. G. and Medeiros A. C., The effect of the rochagan<sup>TM</sup> on radiolabeling with  $^{99\text{m}}\text{Tc}$ . *Cell. Mol. Biol.* 2009, **55**: 23-28.
26. Oliveira C. M., Dantas A. L. A. and Dantas B. M., A methodology to evaluate occupational internal exposure to fluorine-18. *Cell. Mol. Biol.* 2009, **55**: 29-33.